

Summer 7-14-2019

DESIGN AND FABRICATION OF PEEL-OFF AND STICK ANTENNAS

Jayakrishnan Vijayamohanam
University of New Mexico - Main Campus

Follow this and additional works at: https://digitalrepository.unm.edu/ece_etds



Part of the [Electrical and Computer Engineering Commons](#)

Recommended Citation

Vijayamohanam, Jayakrishnan. "DESIGN AND FABRICATION OF PEEL-OFF AND STICK ANTENNAS." (2019).
https://digitalrepository.unm.edu/ece_etds/465

This Thesis is brought to you for free and open access by the Engineering ETDs at UNM Digital Repository. It has been accepted for inclusion in Electrical and Computer Engineering ETDs by an authorized administrator of UNM Digital Repository. For more information, please contact amywinter@unm.edu.

Jayakrishnan Vijayamohanam

Candidate

Electrical and Computer Engineering

Department

This thesis is approved, and it is acceptable in quality and form for publication:

Approved by the Thesis Committee:

Dr Christos Christodoulou, Chairperson

Dr Mark Gilmore

Dr Firas Ayoub

**DESIGN AND FABRICATION OF PEEL-OFF AND STICK
ANTENNAS**

by

JAYAKRISHNAN VIJAYAMOHANAN

**B.TECH, ELECTRONICS AND COMMUNICATION
ENGINEERING, AMRITA VISHWA VIDYAPEETHAM
UNIVERSITY, 2013**

THESIS

Submitted in Partial Fulfillment of the
Requirements for the Degree of

**Master of Science
Electrical Engineering**

The University of New Mexico
Albuquerque, New Mexico

July 2019

Dedication

To Acchan, for always teaching me to be a better person,

To Amma, for all her sacrifice and love,

And to Chettan, for being there whenever I needed him.

Acknowledgement

I would like to sincerely thank Professor Christodoulou for his constant support, encouragement and guidance throughout the last few years of my research and study. Without him this project would not have been conceived and have had so much work done.

I would like to thank Dr. Firas Ayoub for the countless explanations and teachings he was always willing to provide. His friendship and guidance provided a constant push to get this work done.

I would also like to thank Professor Gilmore for his help. He has always been kind to me, and I appreciate his taking time to be on my committee.

I am also thankful to everybody at the Antennas and RF lab for creating a positive work environment and making it a joy to be able to work there.

Design and Fabrication of Peel-off and Stick Antennas

by

Jayakrishnan Vijayamohan

B.Tech, Electronics and Communication Engineering, Amrita School of
Engineering, 2017
M.S., Electrical Engineering, University of New Mexico, 2019

ABSTRACT

Antennas on multiple platforms with the capability to be reused is a novel concept in antenna technologies. This thesis explores the idea of such a flexible antenna that can be stuck on any surface using certain adhesives and be peeled off for reuse for a different purpose. This thesis specifically focuses on the application of being used on small Unmanned Aircraft Systems (sUAVs). Three basic designs are fabricated and investigated. One of them is a reconfigurable meandering monopole, consisting of a PIN diode which resonates at two different frequencies depending on the applied external voltage. A challenge that is addressed is the need for the antenna to be miniaturized, since the frequencies used by sUAVs traditionally require large antennas. To tackle this problem a high bandwidth Log Periodic dipole array (LPDA) is designed and tested. The elements of the LPDA are folded, and the effect this has on the antenna performance is studied. The Q factor for such an antenna is evaluated and correlated as a function of how well the antenna was miniaturized. All the fabricated antennas are tested on multiple surfaces, some of them even conformal, to see how their properties change when stuck to different surfaces.

Contents

List of Figures	viii
Chapter 1 – Introduction	1
1.1 Overview	1
1.2 Organization.....	2
Chapter 2 – Antenna miniaturization theory	4
2.1) Small antennas and their relationship with Q	5
2.2) Computation of Q	7
2.3) Techniques to miniaturize	8
2.3.1) Slot loading.....	8
2.3.2) Bending or folding.....	10
2.3.3) Loading	11
Chapter 3 – Antenna design.....	13
3.1) Design 1 – An annular ring monopole.....	13
3.2) Design 2 – Reconfigurable meandering monopole antenna	15
3.3) Log Periodic Dipole Antenna	18
3.3.1) Design 1 – Bandwidth 1-2 GHz.....	19
3.3.2) Design 2 – Bandwidth 300 MHz – 1.4 GHz.....	23
3.3.3) Q factor optimization.....	26
Chapter 4 – Fabrication.....	28

4.1) Adhesive	28
4.2) Feeding	29
Chapter 5 – Results and discussions	32
5.2) Reconfigurable meander monopole.....	33
5.3) Log periodic dipole array	38
Chapter 6 – Conclusion.....	44
Appendix A – Particle Swarm Optimization	45
A.1 Theory	45
A.2 MATLAB Code	47
References.....	51

List of Figures

Figure 1- Chu sphere of radius 'a' centered about the origin. [5]	5
Figure 2- Chu's limit plotted as a function of 'ka'	6
Figure 3- Schematic showing the parameters of the slot in the patch [9]. Different values for w and l were studied to see how they affect the resonance.....	9
Figure 4 - Example of a meandered dipole with multiple folds.[10]	10
Figure 5 - Slot antenna loaded with two capacitors.[11]	11
Figure 6- The annular ring monopole antenna.....	13
Figure 7- Return loss simulations when the antenna is placed on different surfaces.....	14
Figure 8- Radiation pattern for the annular monopole at 1.75 GHz, showing a peak realized gain of 1.51 dB	15
Figure 9 - Figure showing all elements of the reconfigurable meandered antenna, a) The top layer, and the b) the bottom layer	16
Figure 10- Return loss simulations for the antenna with the diode in both ON and OFF state.	17
Figure 11- The radiation pattern for the meandered monopole antenna in both - a) ON and b) OFF state. The difference in the peak gain and the pattern can be seen.	17
Figure 12 - The schematic of a LPDA showing all the details.	18
Figure 13 - Computed contours of constant directivity versus σ and Γ for LPDA arrays.	20
Figure 14 - Figure showing the alternating elements of the LPDA, black elements being on top plane and the ones in red being placed on the back with a separate feed line there too.	21
Figure 15- Simulation showing return loss for the LPDA design to function from 1-2 GHz.....	22
Figure 16 - Radiation field for the LPDA showing end fire pattern with a peak gain of 6.05 dB .	23
Figure 17- The printed LPDA having meandered elements	24

Figure 18- The return loss Simulation of the printed LPDA with bandwidth 0.3-1.4 GHz.....	25
Figure 19- Radiation pattern for the LPDA at 500 MHz	25
Figure 20 - Change in the Q with successive iterations of PSO	26
Figure 21- The Quality factor of the LPDA before and after applying the PSO	27
Figure 22 - Simulation showing how the SMA is inserted, a) shows the main pin going all the way through and connecting to the bottom feed, and b) shows the ground of the SMA connected to the feed line on top.....	29
Figure 23 - The UFL connector with the surrounding strips being the ground on all four sides. [19].....	30
Figure 24 - The adapter to connect SMA to UFL [19]	30
Figure 25 - Return loss for the annular monopole of radius- 12mm.....	32
Figure 26- The annular monopole when stuck on multiple surfaces	33
Figure 27 – Return loss when monopole is stuck on a beaker	33
Figure 28- a) The front side of the meandered monopole; the backside b) before peeling off, and c) after peeling off.....	34
Figure 29-The return loss for the Antenna in both ON and OFF state	34
Figure 30- Radiation pattern for the Meandered monopole at the ON state, for theta = 0°, at 1.23 GHz.....	35
Figure 31 - Radiation pattern for the Meandered monopole at the ON state, for phi = 90°, at 1.23 GHz.....	35
Figure 32 - Radiation pattern for the Meandered monopole at the OFF state, for phi=90°, at 2.04 GHz.....	36
Figure 33 - Radiation pattern for the Meandered monopole at the OFF state, for theta=0°, at 2.04 GHz.....	36

Figure 34 - The meandered monopole stuck on the surface of a beaker filled with water. 37

Figure 35 - Return loss for the meandered monopole with the antenna stuck on an empty beaker.
..... 37

Figure 37- Return loss of the LPDA showing a bandwidth of 1-2 GHz..... 39

Figure 38 - The LPDA having an affected bandwidth when stuck on cardboard and ceramic tile.
..... 39

Figure 45 - Return loss for the LPDA when stuck to Garolite..... 43

Chapter 1 – Introduction

1.1 Overview

Antennas which can be used on multiple surfaces and multiple times without hindering the device performance is a novel concept in antenna technology. Such a possibility of being able to place an antenna on any surface and peel it off for reuse is the principle subject of this thesis. The antenna can be a single element or an entire array to accommodate various functionalities for various applications and missions. Various reconfigurations on thin printed materials will also allow such light-weight antennas to display various modes of operation and it eliminates the need for multiple antennas for example on small mobile terrestrial or aerospace platforms.

Most UAV (Unmanned Aerial vehicle) systems have limited space and unchangeable geometries that are crucial to their maneuverability. The peel off and stick antennas being discussed in this thesis can satisfy the need for an interchangeable antenna without disrupting the aerodynamic performance by sticking them on the surface.

The performance of such an antenna depends severely on the background, which in this case includes the surface on which it is being stuck. Also, if the antenna is to be stuck on a UAV system, then this surface is likely to be conformal. Thus, the peel off and stick antennas need to adhere well to curved structures, and this can be achieved by fabricating the antennas on thin substrates which can be bent easily.

Small Unmanned Aircraft Systems (sUAS) are a type of unmanned aerial vehicles which are larger than the commonly used hobbyist-drones and are used for military and commercial purposes. The constraint regarding using peel off antennas for such types of aircraft systems is that the sUAVs (Small Unmanned Aerial Vehicles) use very low frequencies (starting from 250 MHz) to communicate.[1] Traditional antennas operating in these frequency ranges can be huge. Thus, there is a need to miniaturize these antennas.

Another aspect worth considering is the feeding mechanism for such antennas. The technique to feed should be easy to connect the transceiver that is already installed. At the same time, the integrated feed network should either be a part of the peel off and stick antenna, or easy to connect to it. For different platforms, appropriate feeding networks can be used.

Apart from sticking on a sUAV, peel and stick antenna can have many other applications such as being stuck on automobile windows, plastic enclosures, and even be used as RFID tags. Their notable attraction is their reusability, as once their purpose is completed it can be peeled off for another function on some other surface.

1.2 Organization

This thesis is divided into the following chapters. It starts with a very brief literature review in Chapter 2 on the various techniques developed to miniaturize antennas. This is relevant since one of the techniques discussed is later used in the design process and is discussed in the results. Also, the Q factor of an antenna is

defined in this Chapter, which is used to show how effective the miniaturization process is in later chapters.

The design procedure involved in this thesis has its roots in identifying the type of antennas that would work within our constraints and fulfill the requirements at the same time. The theory behind the design along with the simulations of all the antennas have been detailed in Chapter 3. The fabricated antennas were then stuck on different surfaces and had its radiation properties measured. Details about the adhesive, peel off process, and the feeding along with all the results are discussed in Chapters 4 and 5 respectively.

An ideal end product in this thesis being discussed would be a sticker type antenna that can be stuck on any surface and be peeled off after use for another function. The antennas would be thin and will be built using flexible substrates so as to increase the adhesion on conformal surfaces. Finally, all the work has been concluded and the future research pathway has been detailed in Chapter 6.

Chapter 2 – Antenna miniaturization theory

One very significant and important research pathway in antennas is miniaturization – how to effectively reduce the antenna size without affecting its performance. There is always a significant need in industry to reduce the size of all components, and one very important study in the field is antenna miniaturization.

A lot of research has been done as to how small antennas can get, and this is explained with the theoretical limits set by Chu [2], as mentioned in 2.1 along with how an electrically small antenna is defined. Later in 2.2, we cover some work done by Yaghjian [3] in how to derive the Q factor of the antennas and this is used later in the results to obtain the Q factor of our antenna. This value is compared to the theoretical threshold and optimized to obtain the best miniaturized antenna. The practical challenge though is that the antenna performance, or the resonant frequency of the antenna depends on the size and hence some innovating techniques need to be applied so as to reduce its electrical length without affecting the resonance, which will be seen in 2.3. Each of the techniques to miniaturize also affects the antennas performance in some way, and hence there will always be a trade-off between the parameters of the antenna.

2.1) Small antennas and their relationship with Q

The first definition of an Electrically small antenna (ESA) was given by Wheeler [4], in which he defined it as an antenna whose maximum dimension is less than $\lambda/2\pi$.

Alternatively, Chu [2] defined the ESA as an antenna that satisfies the condition—

$$ka < 0.5$$

Where k is the wavenumber ($2\pi/\lambda$), and a is the radius of the minimum size sphere that encloses the antenna. This is commonly referred to as the “Chu sphere” and is shown in Figure 1.

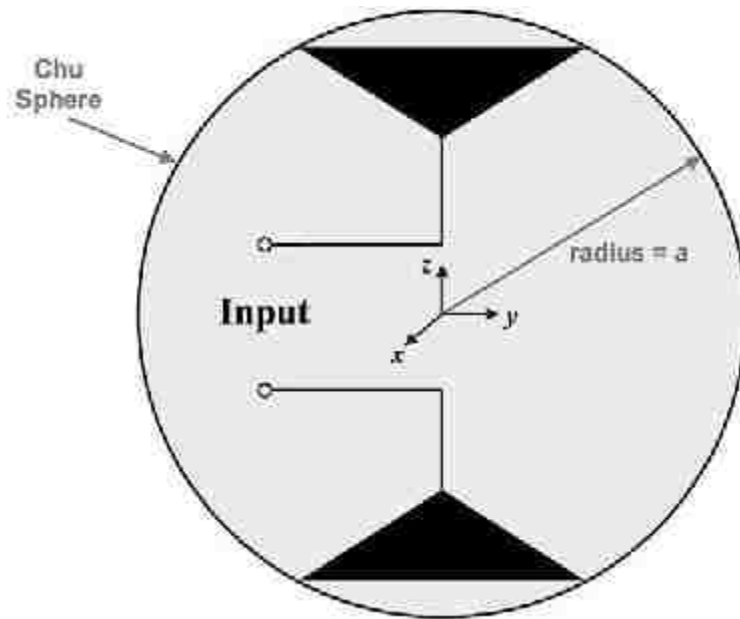


Figure 1- Chu sphere of radius 'a' centered about the origin. [5]

This definition has also extended for the limit to be less than 1. The parameter that is of most interest for these miniaturization studies is Q , or the Quality factor.

In antenna theory, it is defined as –

$$Q = \frac{2 \omega_0 \max(W_E, W_M)}{P_A}$$

Where W_E and W_M are the time averaged stored electric and magnetic energies, and P_A is the received power. Here the antenna considered is resonant at ω_0 .

It is also observed that Q of an antenna is inversely proportional to the bandwidth.[6] The reason Q is so important is this exact relationship, which make it easier to study miniaturization. By studying the Q values of our antennas, we can derive our bandwidth. Hence if there were to be a fundamental lower limit on how small Q could be, that would result in the optimum or maximum bandwidth that particular configuration could achieve. Collin and Rothschild [7] worked out a limitation on Q given below, which was later confirmed by others.[8][9]

$$Q = \frac{1}{k^3 a^3} + \frac{1}{ka}$$

This Q value is plotted in Figure 2 and represents the lowest value which can be theoretically obtained, also called as *Chu's limit*.

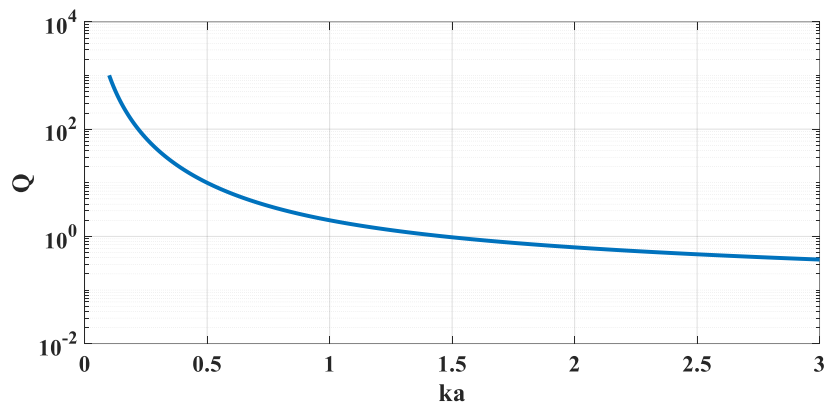


Figure 2- Chu's limit plotted as a function of 'ka'

2.2) Computation of Q

A key contribution in miniaturization theory was given by Yaghjian and Best[3] - they derived a new expression for Q in terms of input impedance, and which is valid for all frequencies. The validity and accuracy of the derived expressions were also confirmed with numerical data of several antennas.[3]

To derive the expression, the radiation resistance of the antenna is modelled into a series RLC circuit for a resonance or into a parallel RLC circuit in antiresonance.

The antennas input impedance can be written as

$$Z_0(\omega) = R_0(\omega) + jX_0(\omega)$$

$R(\omega)$ is the input resistance and the real number $X(\omega)$ is the input reactance of the antenna.

The frequency ω_0 , at which $X_0(\omega_0) = 0$, defines the resonant frequency of the antenna if $X_0'(\omega_0) > 0$ and as the antiresonant frequency if $X_0'(\omega_0) < 0$.

He goes on to evaluate the dispersion energies associated with dissipation W_L and radiation W_R using such a model. They conclude that Q can be accurately represented throughout all frequency ranges by -

$$Q(\omega_0) \approx \frac{\omega_0}{2 R_A(\omega_0)} |Z'_{in}(\omega_0)|$$
$$= \frac{\omega_0}{2 R_A(\omega_0)} \sqrt{(R'_A(\omega_0))^2 + \left(X'_A(\omega_0) + \frac{|X_A(\omega_0)|}{\omega_0} \right)^2}$$

The significance of this equation lies in the fact that using it, the Quality factor of an antenna can be determined just using the complex input impedance. This is later used to determine the Q for our antennas.

2.3) Techniques to miniaturize

In this section a review on some of the techniques being used to design small antennas is briefly covered.

2.3.1) Slot loading

In this technique slots are cut into the metal patch with the purpose of alternating current flow. The slots create a longer electrical path for the current to travel, hence affecting the effective electrical length of the antenna. To show this Nguyen [10] investigated the effect of slot length on a patch antenna, as shown in Figure 3.

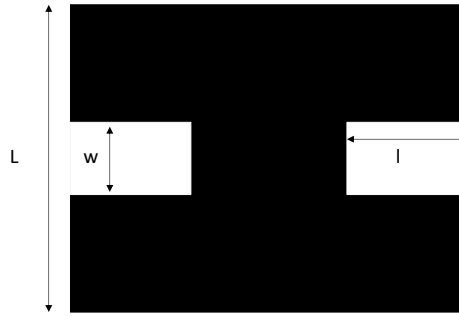


Figure 3- Schematic showing the parameters of the slot in the patch [9]. Different values for w and l were studied to see how they affect the resonance.

The original patch (with no slots) is set to resonate at 1.5 GHz. As expected, Nguyen was able to show that the resonant frequency decreased as he increased the notch length and width respectively. The results are summarized in Table 1 and 2.

Frequency	l ($w=5\text{mm}$)
1.37	10
1.24	15
1.10	20
0.887	26.33

Table 1-- Table showing how the resonant frequency changes for different values of l , with $w=5\text{mm}$ kept constant.

Frequency	w(l=26.33mm)
0.96	1
0.85	8
0.8	15
0.77	20

Table 2- Table showing how resonant frequencies change for different values of w, with l=26.33 kept constant.

2.3.2) Bending or folding

Using the same logic of creating slots, bending or folding the antenna would increase the distance the current has to travel and hence is another way to miniaturize the antenna. The PIFA antenna is a classic example of this and is already used in many wireless devices. This can be also extended to many folds, thus resulting in meandered antennas, as shown below in Figure 4.

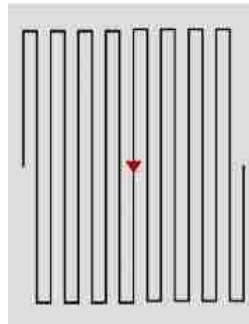


Figure 4 - Example of a meandered dipole with multiple folds.[10]

This particular meandered dipole shown can be enclosed within a sphere of $ka=0.499$ and resonates at 543.33 MHz. A conventional dipole within the same size sphere would radiate at 1.73 GHz. The meandered monopole is also in principle equivalent to an inductively loaded monopole, with the gaps in between

consecutive folds being modelled as inductors in the equivalent circuit of the antenna.[11]

2.3.3) Loading

Both folding an antenna and having slots can be explained using lumped loading. In effect, both the methods consist of adding some amount of inductance or capacitance to the antenna. However, there are many other ways to do this as well. High contrast materials at certain locations can be placed to achieve this. Or lumped elements like capacitors can be used, as shown in Figure 5.

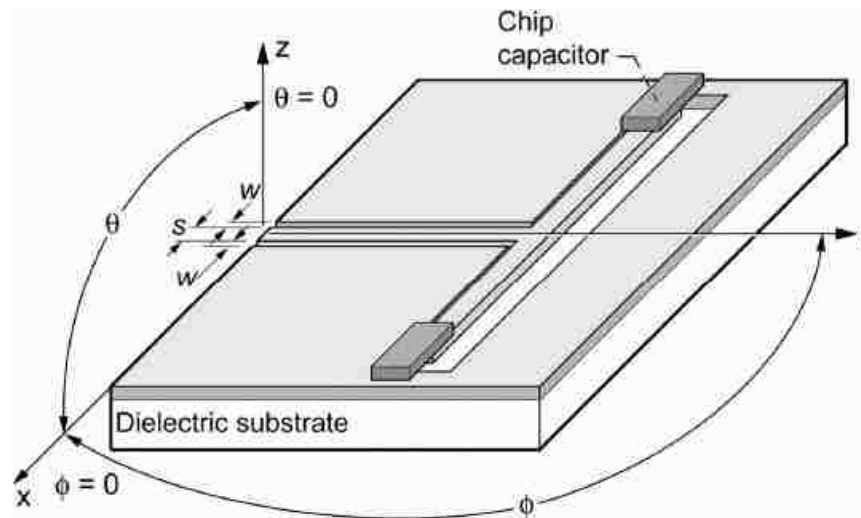


Figure 5 - Slot antenna loaded with two capacitors.[11]

In the work done by Scardelletti [11], a CPW fed slot antenna has two capacitors attached at the ends and is studied. The lumped chip capacitors of 0.8pF were able to reduce the frequency by 22%.

Each of these methods are seen to reduce the resonant frequencies, but at some other cost of affecting the performance of the antenna either in impedance

matching or the maximum gain radiated. Hence for any purpose to miniaturize the antenna, one of the discussed suitable techniques can be applied keeping in consideration the drawbacks.

Chapter 3 – Antenna design

Next, we show designs that have been developed as the best candidates for our peel-off and stick antennas.

3.1) Design 1 – An annular ring monopole

The annular monopole antenna was designed as the first design because of its simplicity and its small size. The radiating region is an annular ring which is fed by a Coplanar waveguide. This makes sure that the entire antenna, both the radiating part and the ground are printed on one side of the substrate. This leaves the adhesive to easily be placed on the bottom without any worries about affecting its performance. The ground in this particular design are two triangular patches surrounding both sides of the feed, as shown in Figure 6. The frequency would depend on the ring of the radius and thus can be adjusted as per the requirements.

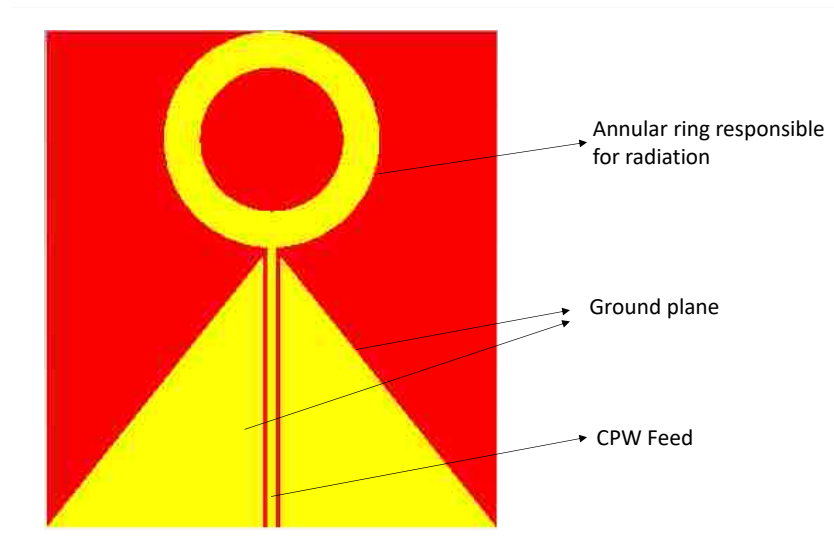


Figure 6- The annular ring monopole antenna

The antenna is initially designed on Computer Simulation Technology (CST) Studio and then tweaked so as to get peak radiation at 1.75 GHz. The resulting radius is 12.5 mm. The substrate used is Rogers 5870, and of thickness 0.13 mm. The simulation results of the S- parameters when the antenna is placed on different surfaces is shown in Figure-7.

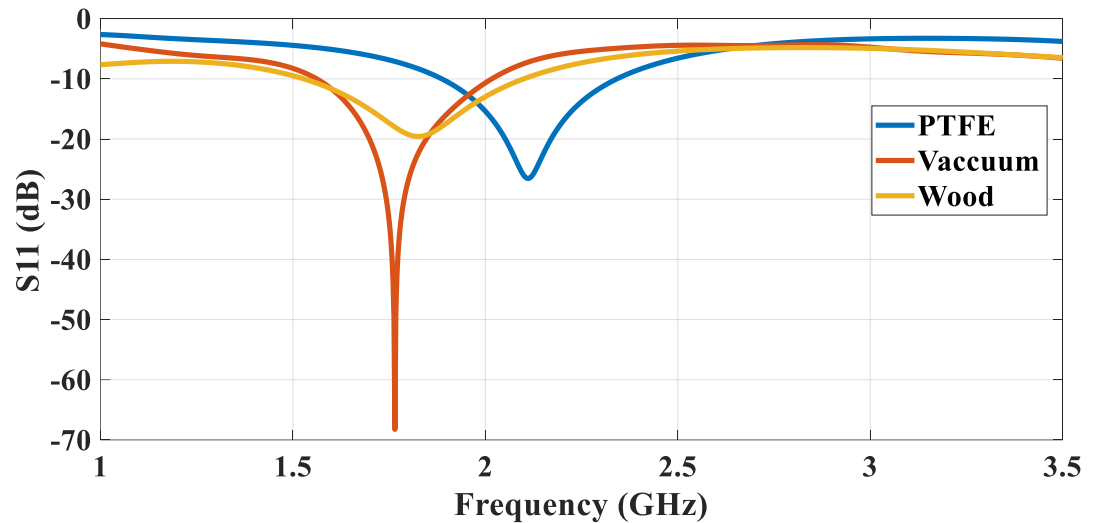


Figure 7- Return loss simulations when the antenna is placed on different surfaces.

The simulation results verified the design, as the resonant frequency was exactly at 1.75 GHz. However, the frequency shifted to higher values when the antenna was stuck on other materials. This can be explained by considering the equivalent circuit of the antenna as an RLC circuit. At resonance, the capacitive and inductive elements cancel out each other, showing the antennas impedance as purely resistive at this frequency. Placing this antenna on the surface of a material, alters this frequency as it adds some reactive elements to the circuit. Hence, the surface on which it is being placed should also be considered while designing a peel-off antenna. The annular ring monopole showed peak matching

for PTFE at 2.14 GHz, and around 1.8 GHz for wood. Thus, a peel off antenna which operates in a single frequency was designed and simulated successfully.

The radiation pattern of the simulation is showed in Figure 8.

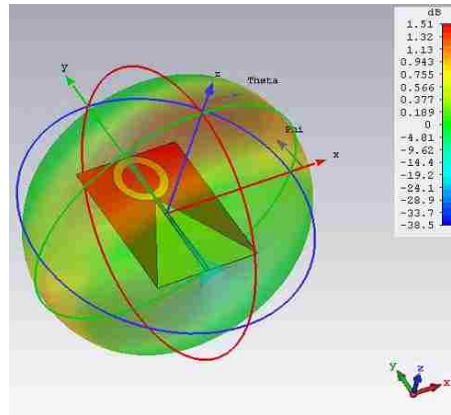


Figure 8- Radiation pattern for the annular monopole at 1.75 GHz, showing a peak realized gain of 1.51 dB

3.2) Design 2 – Reconfigurable meandering monopole antenna

Reconfigurability of antennas in terms of frequency is a desired trait. In terms of aircraft communications, an antenna that operates in two different frequencies (one for uplink and the other for downlink) is better than having two separate antennas. This can be achieved in many ways, one of them by using PIN diodes, which act as two different lumped elements, depending on the external voltage applied. This design consists of a single monopole, which is meandered to reduce its size [13].

The monopole is designed on a 0.5 mm thick Rogers Duroid 5870 substrate with $\epsilon_r = 2.33$ and $\tan \sigma = 0.0012$. The bottom layer consists of a partial ground plane and the meandered monopole lies on the top layer, as shown in Figure 9. The

monopole has three meandered arms of width 2.3 mm. The PIN diode is added to the second arm.

The PIN diode used is an Aluminum Gallium Arsenide Flip Chip diode(model-MA4AGP90) from MACOM and acts as in the ON state as a 0.3 nH inductor in series with a 6 Ω resistor. In the OFF state it acts as a 0.3 nH inductor in series with a 0.02 pF capacitor in parallel to a 10 k Ω resistor. The antenna is simulated in CST and is shown in Figure 9. The two desired frequencies of operation for this design are taken from the bands used to communicate by sUAVs.

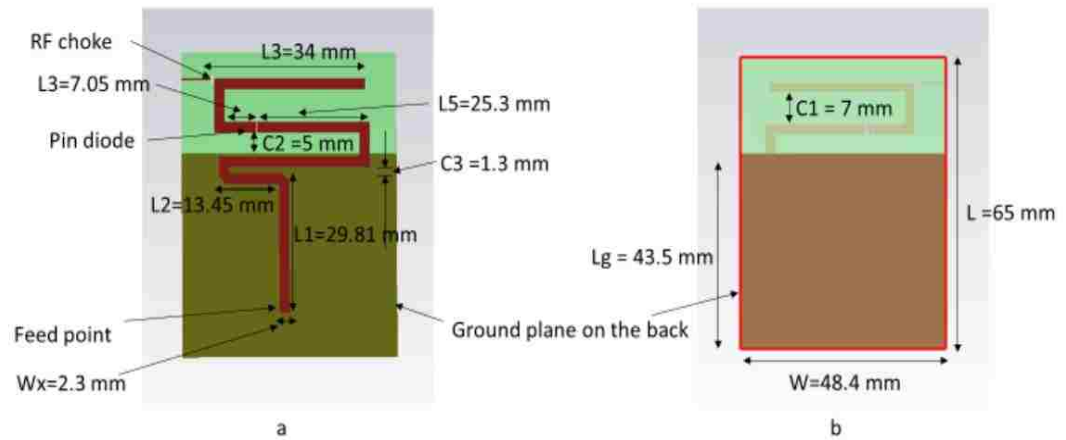


Figure 9 - Figure showing all elements of the reconfigurable meandered antenna, a) The top layer, and the b) the bottom layer

The diode is meant to be controlled by an external voltage fed through a bias-tee connected to the antenna. The diode was modelled as lumped element in CST and the simulation results for both cases are shown in Figure 10.

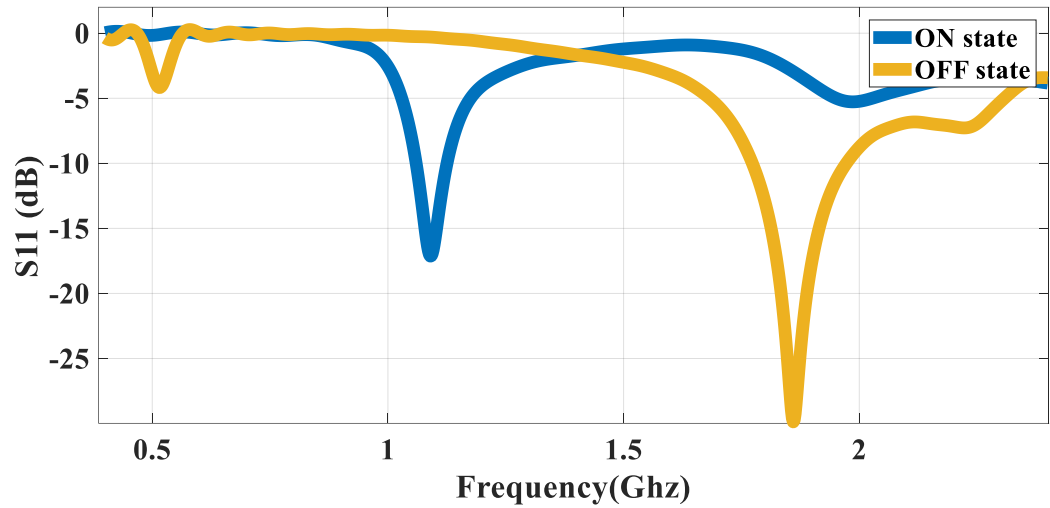


Figure 10- Return loss simulations for the antenna with the diode in both ON and OFF state.

As seen in Figure 10, the antenna works at two different frequencies depending on the diode bias. The antenna was optimized so as to get these two resonant frequencies at 1755-1850 MHz and 1090 MHz, because these two bands are used for transponder uplink and downlink by antennas on sUAVs.

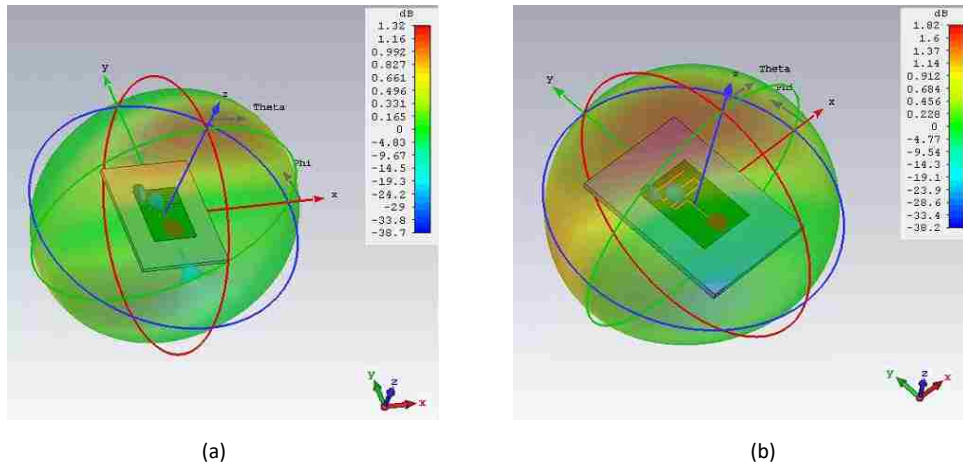


Figure 11- The radiation pattern for the meandered monopole antenna in both - a) ON and b) OFF state. The difference in the peak gain and the pattern can be seen.

3.3) Log Periodic Dipole Antenna

The Log Periodic dipole antenna is a multi-element wide band, directional array. It was introduced by R.H. DuHamel and Isabell [14]. This simple design consisting of an array of linearly placed dipoles exhibits relatively uniform input impedances, VSWR and radiation characteristics over a wide range of frequencies.

The entire array has an active region, i.e. regions where it is radiating or receiving radiation effectively that shifts with frequency. The entire bandwidth of the array depends on the length of the longest and shortest elements. At the lowest usable frequency, the longest element should be resonating and similarly at the highest frequency of the bandwidth the smallest element should be resonating.

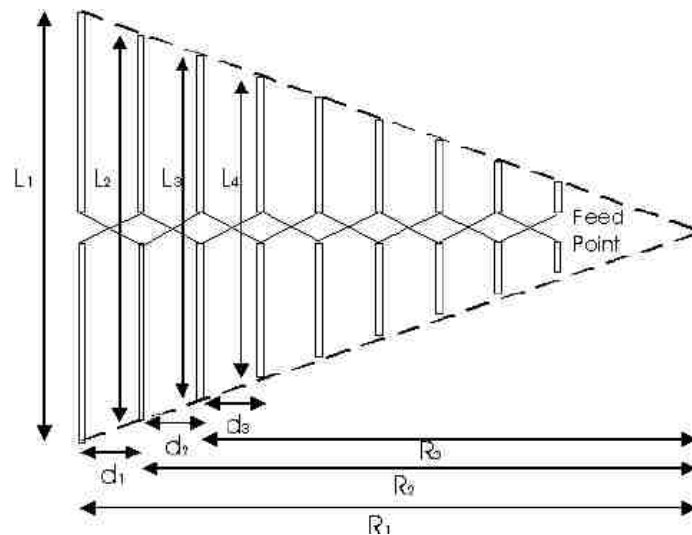


Figure 12 - The schematic of a LPDA showing all the details.

The consecutive elements of the array keep reducing in length according to a scaling factor k . Ideally, all the parameters of the LPDA would depend on k , as –

$$\frac{1}{k} = \frac{L_1}{L_2} = \frac{L_n}{L_{n+1}} = \frac{R_2}{R_1} = \frac{R_n}{R_{n+1}} = \frac{d_2}{d_1} = \frac{d_{n+1}}{d_n} \quad (1)$$

where,

l = length of the elements

R = Distance of the element measured from the feed-point

d = Spacing between the elements

The design procedure of the LPDA was first detailed by Carrel [15]. But it was Pantoja [16], who using the work of Carrel first printed the log periodic array onto a substrate. Pantoja decide to print the elements alternatively on the front and back, to ensure the adjacent elements don't couple. The printed LPDA ensures the same radiation pattern but with a decreased gain value. The same design is considered here, and the design parameters were calculated using the guidelines given by Carrel.

3.3.1) Design 1 – Bandwidth 1-2 GHz

Firstly, the number of elements has to be decided depending on the required gain and the scaling factor to be used while designing. This is done with the help of a contour calculation Carrel has provided [15]. After taking the desired gain as 8 dB the scale factor and the spacing factor is selected as 0.83 and 0.12 respectively from the plot shown in Figure 13.

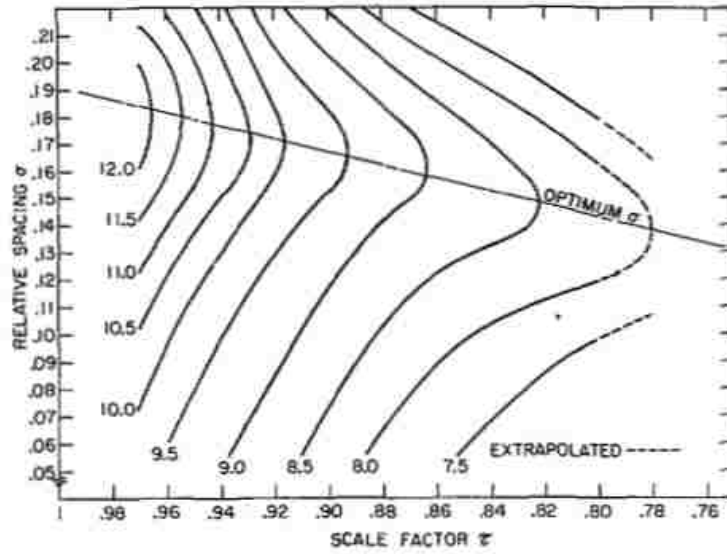


Figure 13 - Computed contours of constant directivity versus σ and Γ for LPDA arrays.

The angle subtended by the array is then decided by the formula –

$$\alpha = \tan^{-1} \left[\frac{1-\tau}{4\sigma} \right] \quad (2)$$

Here τ is the scaling factor, and σ the relative spacing. The angle subtended is used to calculate the effective bandwidth using a semiempirical equation –

$$B_{ar} = 1.1 + 7.7(1 - \tau)^2 \cot \alpha \quad (3)$$

However, in practice a slightly larger bandwidth (B_s) is designed, which is greater than the required bandwidth. Hence,

$$B_s = BB_{ar} = B[1.1 + 7.7(1 - \tau)^2 \cot \alpha] \quad (4)$$

where

B_s = designed bandwidth

B = desired bandwidth

B_{ar} = active region bandwidth

For our first design the values were calculated and found out as $\alpha = 9.48^\circ$, $B_{ar} = B_s = 1.73$. The bandwidth selected is 1-2GHz.

Next, the number of elements were determined using and were found out to be 5, using equation 5 -

$$N = 1 + \frac{\ln(B_s)}{\ln(1/\tau)} \quad (5)$$

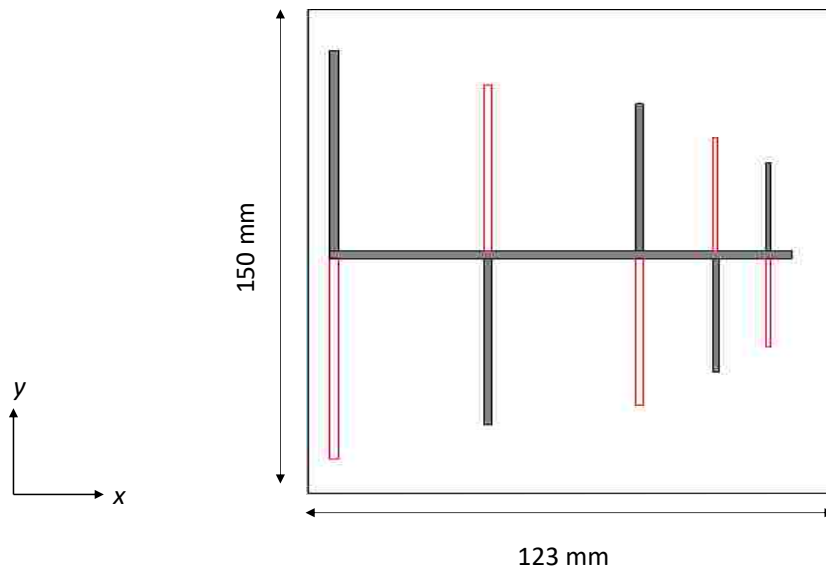


Figure 14 - Figure showing the alternating elements of the LPDA, black elements being on top plane and the ones in red being placed on the back with a separate feed line there too.

Using all this information, the design was modelled as shown in Figure 14. The element lengths were initially decided depending on the spacing factor and the bandwidth, and later optimized. The elements are alternating; the ones in black are on the top plane of the antenna and the ones in red are fed via another feed line placed on the bottom plane of the antenna. This ensures not only that adjacent

elements but makes it easy to fabricate the feeding network. The top side of the antenna can be connected to the main current, and the bottom to the ground to ensure proper phase difference.

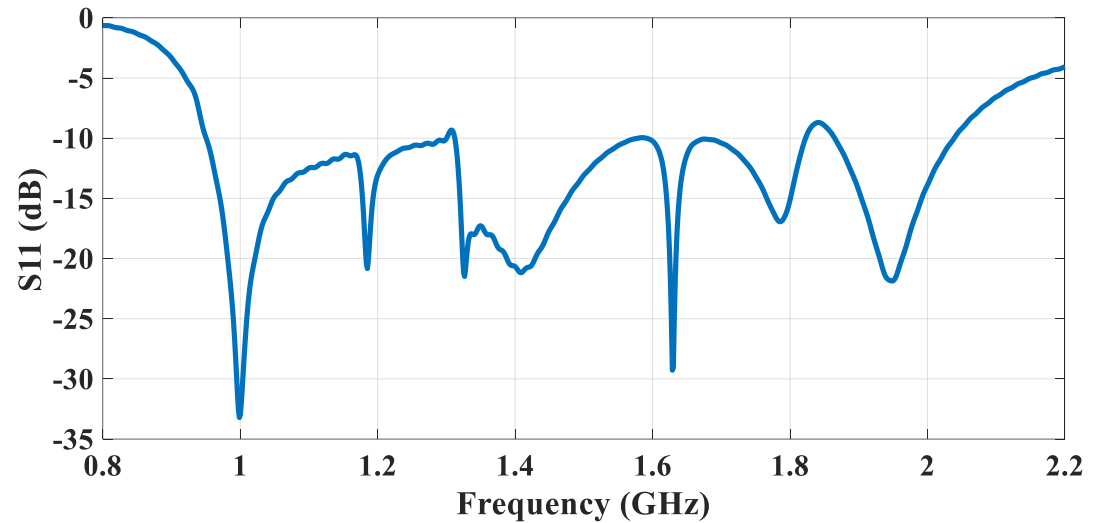


Figure 15- Simulation showing return loss for the LPDA design to function from 1-2 GHz

The simulation results, as seen in Figure 15 show that it is well matched from 1-2 GHz just as we require. The radiation pattern was simulated as seen in Figure 16, and the antenna is seen to exhibit end fire radiation just as the theory predicts.

Both the return loss and the radiation pattern would later be verified by measurements.

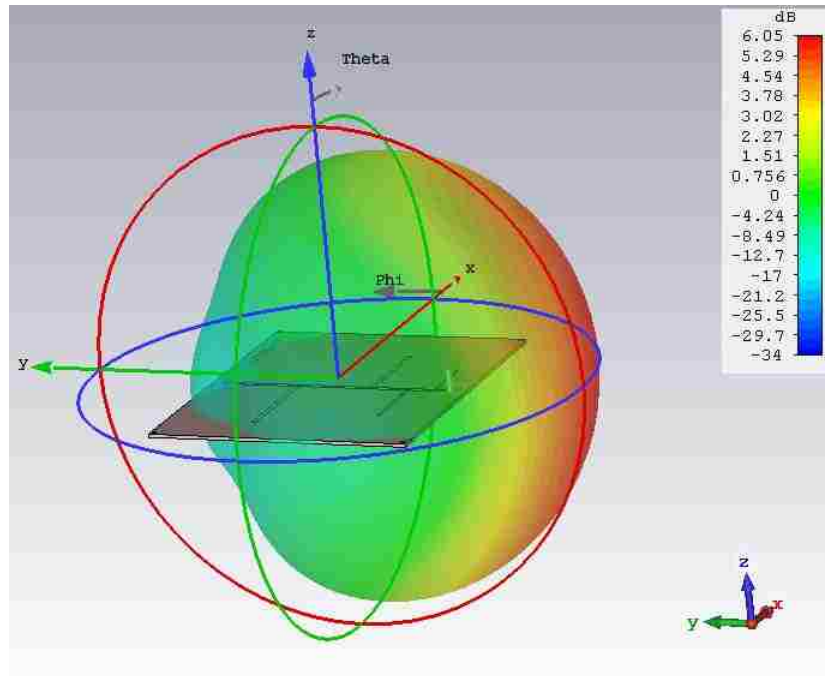


Figure 16 - Radiation field for the LPDA showing end fire pattern with a peak gain of 6.05 dB

3.3.2) Design 2 – Bandwidth 300 MHz – 1.4 GHz

For the application of peel off and stick antennas to be used on sUAVs, it was essential that frequencies be identified that such aircraft systems utilize. Many of the sUAVs utilize smaller frequencies lower than 500 MHz [1]. The transponder used by BAE drones and TICK frequency allocated by the NTIA (National Telecommunications and Information Administration) is 1090 MHz [17]. Hence a peel off antenna to be stuck on any sUAV would ideally need to be covering all these bands. Thus, here a LPDA array for the very same purpose is designed.

The problem with covering such frequencies is that the size of the antenna becomes too large. The radiation of a dipole only occurs when the length of the whole dipole is equal to half the wavelength of the wave. Hence for a dipole to radiate at 300 MHz, the length of it has to be 50 cm.

Hence there is a need to miniaturize the antenna elements involved, and this can be done in many ways, as discussed in Chapter 2. For our design, we decide to fold each of the elements of the LPDA. The parameters for the design are calculated by the equations used before, and the design is shown in Figure 17.

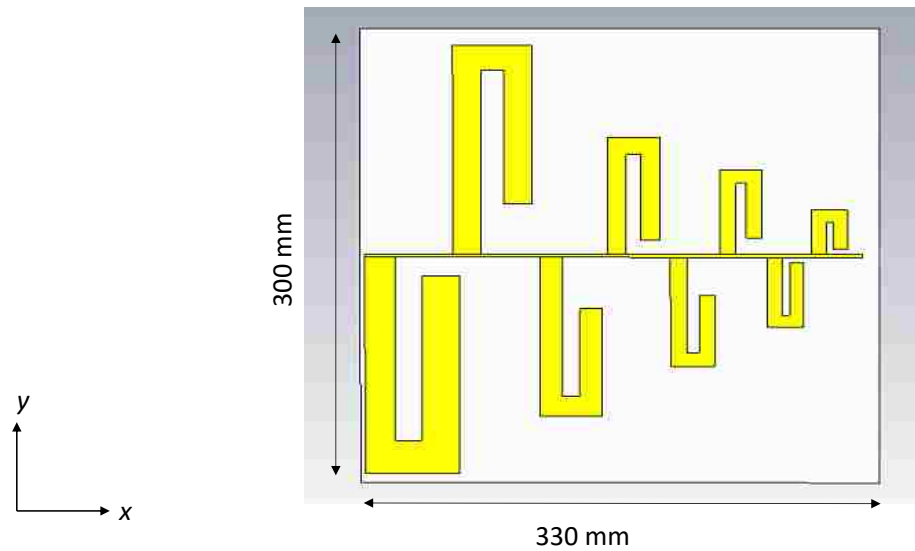


Figure 17- The printed LPDA having meandered elements

The design is later optimized in CST and is shown in Figure 6, where each element is meandered as a folded dipole.

The return loss is shown in Figure 18, and we can clearly see that the antenna has a -10dB bandwidth from 320 to 1400 MHz. The length of the largest element is 143 mm, which is a 39% reduction from the standard length to radiate at 320 MHz. Also, the Q factor of the antenna and its relation was studied, as explained in Chapter 4.

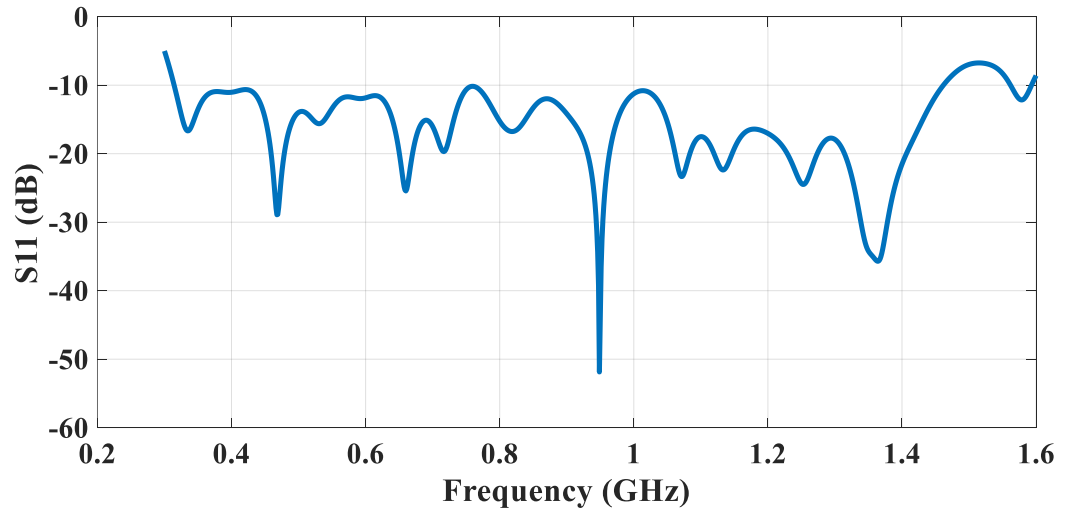


Figure 18- The return loss Simulation of the printed LPDA with bandwidth 0.3-1.4 GHz

The radiation pattern for the antenna was also simulated, as shown in Figure 19. It was observed that meandering the elements caused the gain of the array to drop.

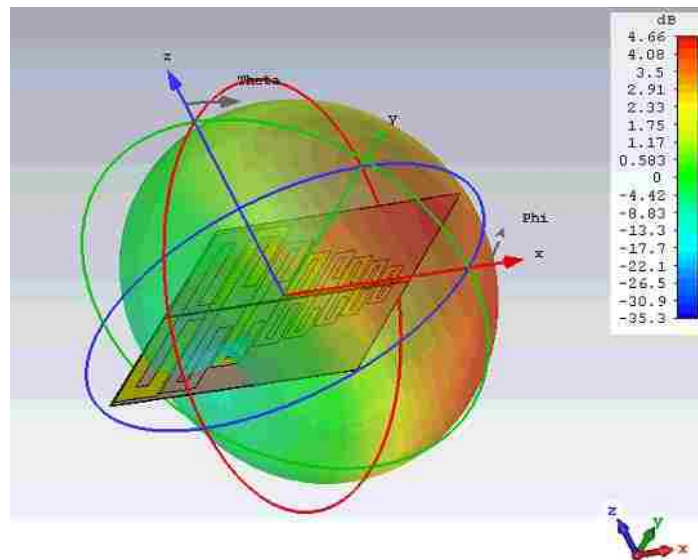


Figure 19- Radiation pattern for the LPDA at 500 MHz

The decrease in gain can probably be attributed to the meandering causing some coupling between the elements of the array, which in turn hampers the radiation.

3.3.3) Q factor optimization

Since meandering the LPDA effectively miniaturizes the antenna, the Q factor was evaluated for the antenna using formula 2.4. As discussed in Chapter 2, a lower Q value indicates a higher effective miniaturization in terms of radiation efficiency and bandwidth. Hence an optimization was applied to reduce the Q throughout the frequency range. CST was linked to MATLAB, and a particle swarm optimization algorithm (described in Appendix) was applied to a swarm size containing all the possible values for the parameters of the LPDA. The algorithm was allowed to run for 501 simulations, and the decrease in the average Q value is shown in Figure 12. Also, the entire range was compared with the beginning of the optimization, as seen in Figure 13.

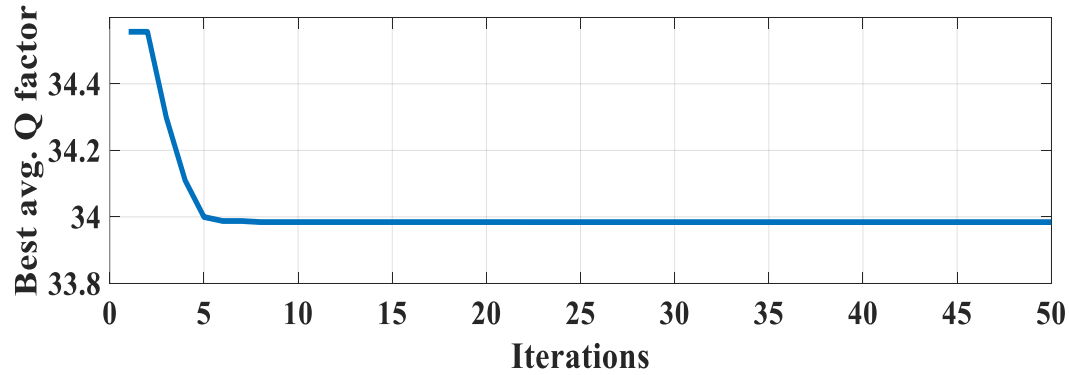


Figure 20 - Change in the Q with successive iterations of PSO

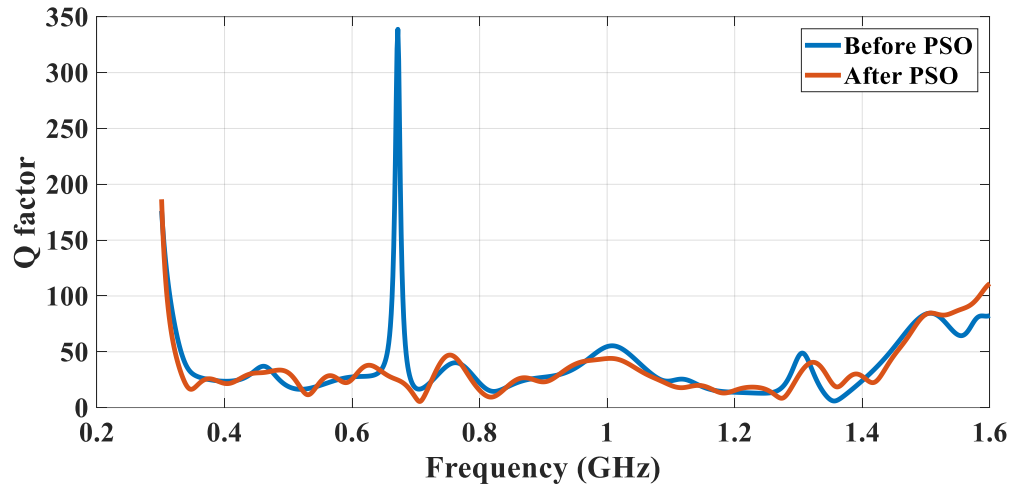


Figure 21- The Quality factor of the LPDA before and after applying the PSO

The figure shows that certain high peaks in the Q factor was able to be decreased by the optimization. We can clearly see that one spike in the Q factor close to 700 MHz was able to be nullified using PSO.

Chapter 4 – Fabrication

4.1) Adhesive

Adhesives are defined as specific substances that when applied to two different objects binds them together, either temporarily or permanent. Adhesives are both - found in nature and also produced synthetically. Currently it has a ubiquitous presence and has profound impact on several products that we use.

Among the different adhesives found in the market, for our purpose we decided to use Pressure sensitive adhesive (PSA) tapes as the back lining of our antennas.

These tapes wet the surfaces in contact and create bonds when adhered by some initial pressure.[18] The adhesive component in such tapes are rubber, acrylic or silicone. There are chances of faults such as bubbles or detachment which can occur if the pressure is not high enough, or even if the external factors such as temperature or humidity is unsuitable. Also, the tolerance of sustaining high loads is not much.

The advantages that such PSA tapes offer over other types of adhesives is that they are relatively thin flexible materials, which can have two different adhesive coatings on both the sides (one for permanent adhesion, and the other for repeated usage). The composition consists of the adhesive sandwiched in between the release liner and the carrier.

The products used for our design were MACTAC FBT360 and Double bond – differential tape. Both the tapes were stuck to the substrates in consideration and kept in an oven for temperature testing. Both the tapes went through no damage up to 125° C. Also, the antennas made were checked for repeated usage using these tapes. They were deemed to be in good condition even after 20-25 attempts of sticking onto PTFE slabs.

4.2) Feeding

For the LPDA antenna the antenna was fed using a SMA connector which could be placed horizontally on top of the design, as shown in Figure 22. The main pin goes through the board and joins the feed line on the bottom plane while the ground of the SMA is connected to the feed line on top. This ensures that both the planes are fed with a phase difference of 180°.

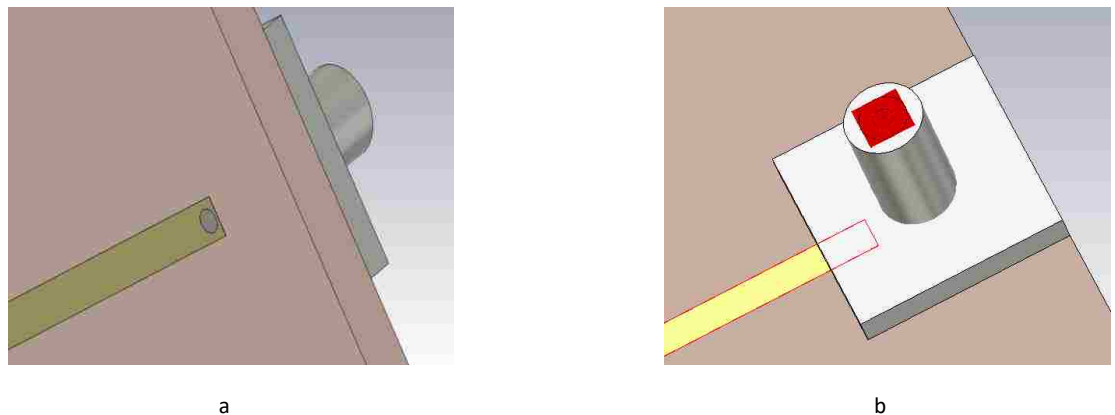


Figure 22 - Simulation showing how the SMA is inserted, a) shows the main pin going all the way through and connecting to the bottom feed, and b) shows the ground of the SMA connected to the feed line on top.

However, this could not be done in the earlier cases since they are made on a very thin substrate. Also, the ground plane is present on the same plane for our first

design. Hence a U.F.L connector, shown in Figure 23 is used for these designs. This UFL holder can be soldered onto the design. It is extremely small, having a size of 2.5 mm X 2 mm. The UFL has the ground on its sides, and hence can be directly soldered onto the CPW fed monopole antenna. The drawbacks for the UFL are that it is not durable, and that it can only be used for up to 3 GHz.



Figure 23 - The UFL connector with the surrounding strips being the ground on all four sides. [19]

It is mostly used where conserving space is the priority, like inside laptops and other embedded systems. For our testing purpose we use the adapter to connect an SMA to UFL, as shown in Figure 24.



Figure 24 - The adapter to connect SMA to UFL [19]

For the meandered reconfigurable monopole, the connector is soldered onto the back side next to the ground, while the main pin goes through and is connected to the feed point. This can be achieved through either the SMA or the UFL, depending on the need.

Chapter 5 – Results and discussions

In this chapter the measured results when the antenna is stuck on different surfaces are compared with the simulations. Some brief simulation results with the Quality factor of the LPDA is also detailed.

5.1 Monopole antenna

The annular monopole ring peel and stick off antenna was fabricated and tested by being stuck on multiple surfaces, as shown in Figure 26. The Feeding was done by soldering on the UFL surface mount holder onto the CPW feed. The monopole ring was fabricated using the LPKF Protolaser S4 on a Rogers 5870 substrate of thickness 0.13 mm. It was then connected to a Vector Network Analyzer and checked for its S parameters. The obtained reflection coefficient along with the simulated results are shown in Figure 25, and the setup in Figure 26.

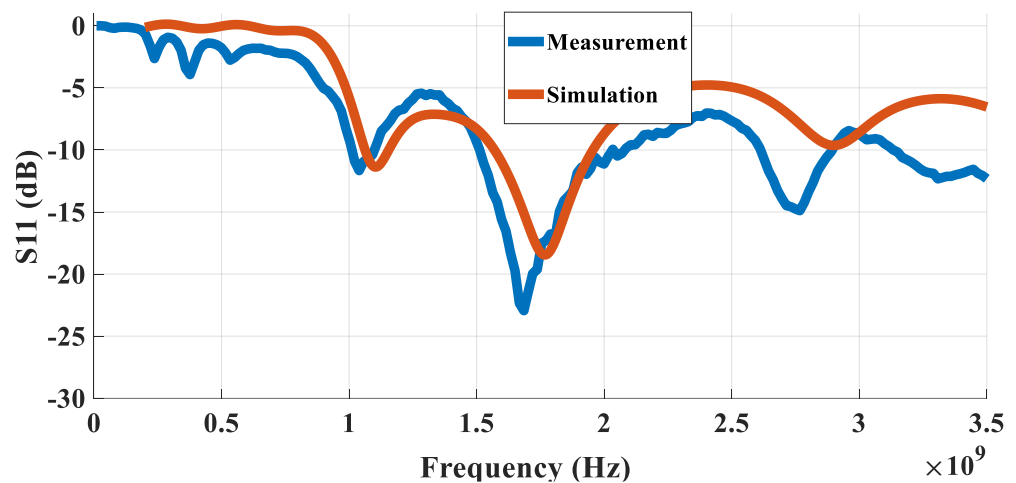


Figure 25 - Return loss for the annular monopole of radius- 12mm



Figure 26- The annular monopole when stuck on multiple surfaces

The antenna is then tested by being stuck on a beaker. The return loss measurements are shown in Figure 29, both with an empty beaker and a beaker filled with water.

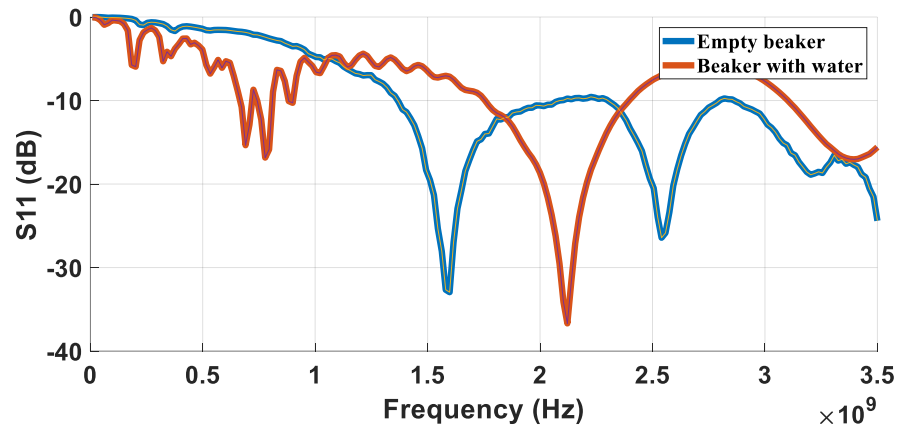


Figure 27 – Return loss when monopole is stuck on a beaker

5.2) Reconfigurable meander monopole

For the meandering monopole the same fabrication procedure was followed, however the UFL holder was used for feeding by being soldered onto the bottom layer below the strip of adhesive, as seen in Figure 22. This antenna was then

stuck onto different surfaces and tested for its resonance using the VNA. An external DC source provided the bias voltage for the pin diode, which was fed along with the help of a bias tee.

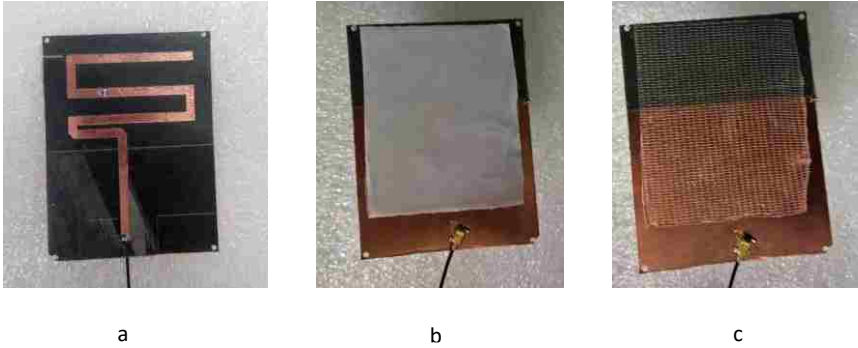


Figure 28- a) The front side of the meandered monopole; the backside b) before peeling off, and c) after peeling off

The response was first taken when stuck on foam and compared to the simulation results, as seen in Figure 15. The diode is given a voltage of 1.3 V from the DC source which is connected to a bias tee at the input side. The antenna measurements seemed to show agreement with the simulations.

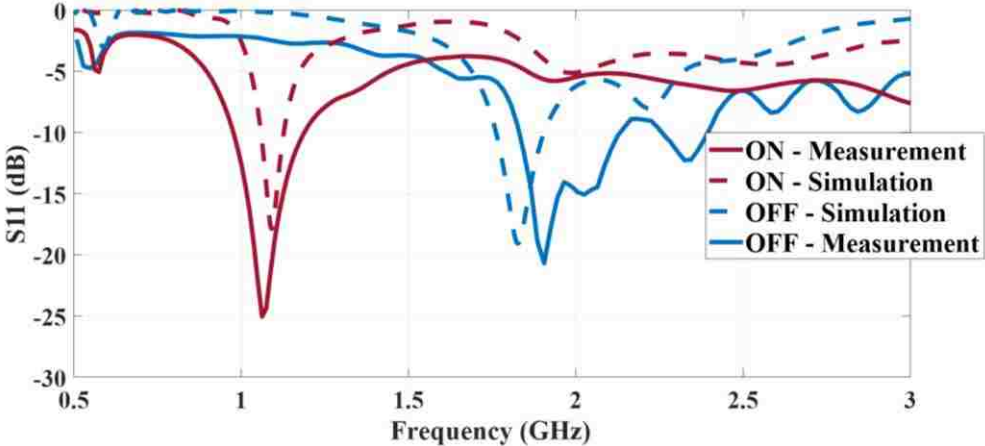


Figure 29-The return loss for the Antenna in both ON and OFF state

The radiation patter was then measured for both the states and compared with the simulation, as seen in Figures 30-33.

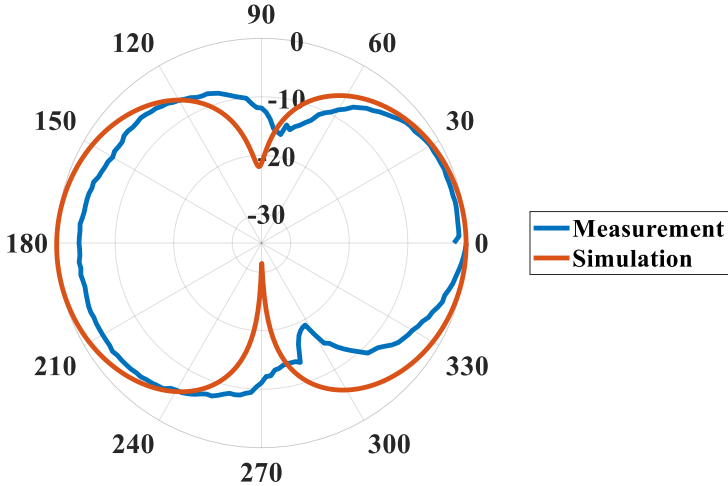


Figure 30- Radiation pattern for the Meandered monopole at the ON state, for $\theta = 0^\circ$, at 1.23 GHz

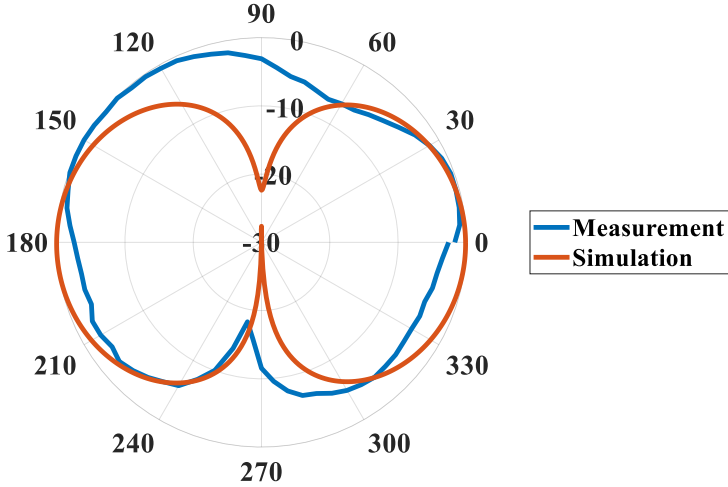


Figure 31 - Radiation pattern for the Meandered monopole at the ON state, for $\Phi = 90^\circ$, at 1.23 GHz

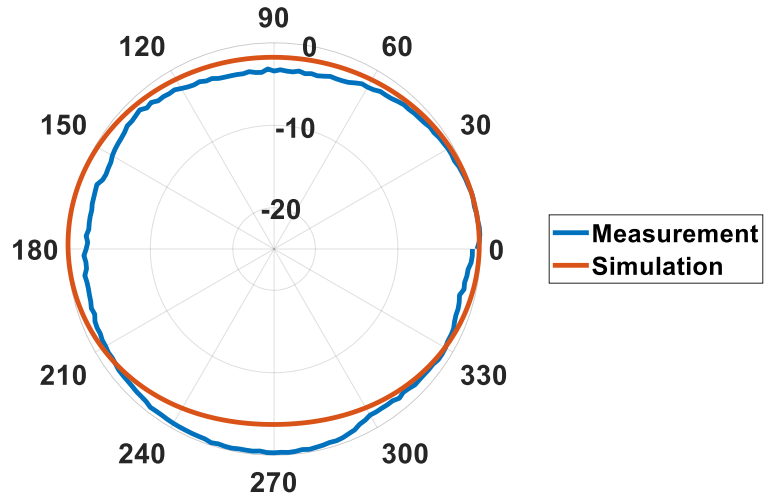


Figure 32 - Radiation pattern for the Meandered monopole at the OFF state, for $\Phi=90^\circ$, at 2.04 GHz.

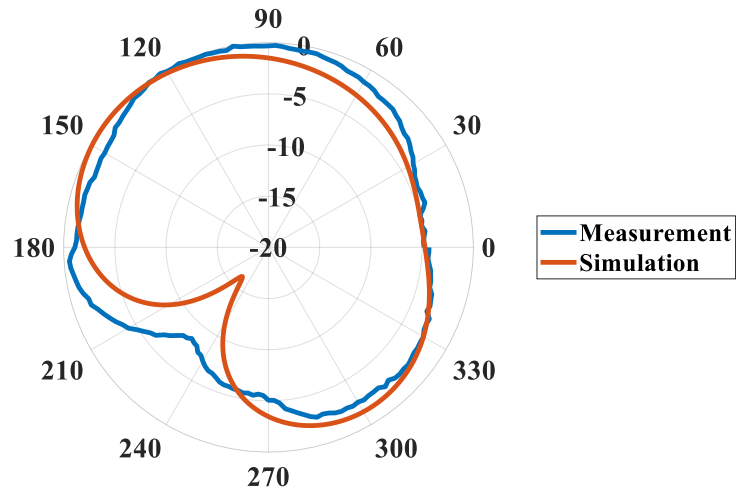


Figure 33 - Radiation pattern for the Meandered monopole at the OFF state, for $\theta=0^\circ$, at 2.04 GHz.

We can see that the antenna radiates omni directional for the $\Phi = 90^\circ$ plane, just as an ideal dipole would. However, we see two nulls in the same plane when the antenna is switched ON, and this is probably caused by the reactance caused by the dipole. For the $\theta=0^\circ$ plane in the OFF state, there is only one null and that too

at 240° which can be explained by the meandering causing the maximum and minimum fields to be oriented in such a way.



Figure 34 - The meandered monopole stuck on the surface of a beaker filled with water.

The performance of the antenna was then checked after being stuck on the surface of a beaker, as seen in Figure 36. The antenna was shown to be functional in both the different states even when stuck on curved surfaces such as the beaker.

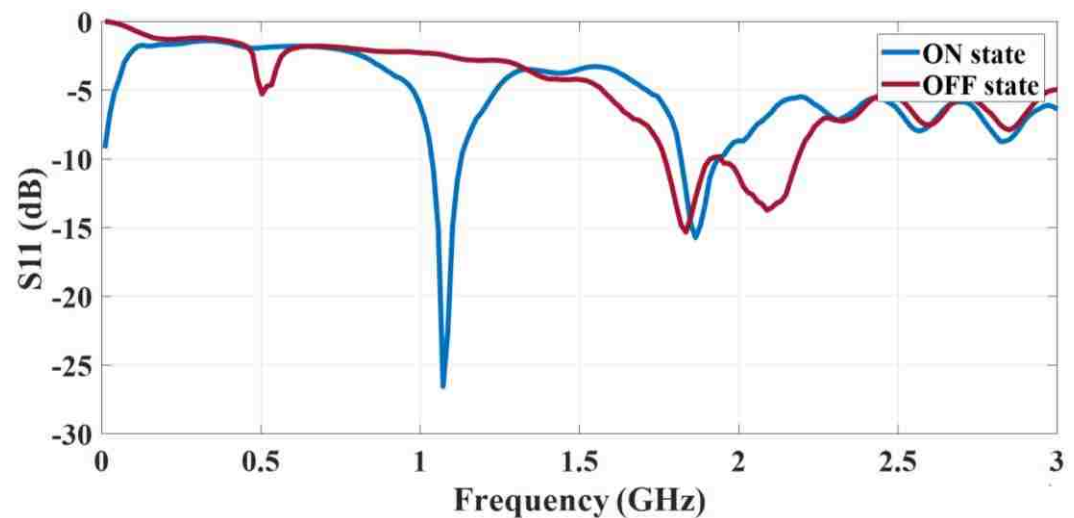


Figure 35 - Return loss for the meandered monopole with the antenna stuck on an empty beaker.

5.3) Log periodic dipole array

The first LPDA design (1-2 GHz) was fabricated using the LPKF Protomat S63 milling machine and stuck on different surfaces as shown in Figure 39.

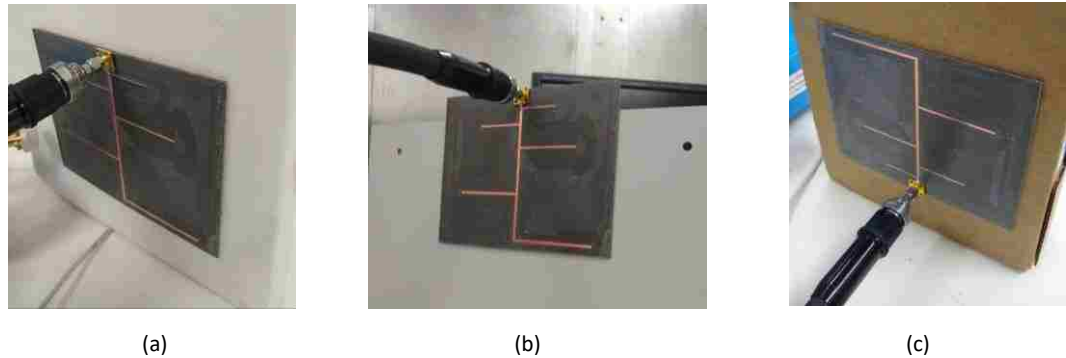


Figure 36 - The LPDA being stuck on a) foam, b) ceramic tile and c) cardboard box

The VNA was connected to a SMA port which was soldered perpendicular to the plane of the antenna. The bandwidth of this fabricated antenna was confirmed by taking the readings sticking it to foam, as seen in Figure 38. The antenna bandwidth was severely hampered by being stuck on the ceramic tile and the cardboard box, as seen in Figure 39. However, this could have been overcome by probably considering the surface along with the antenna while designing.

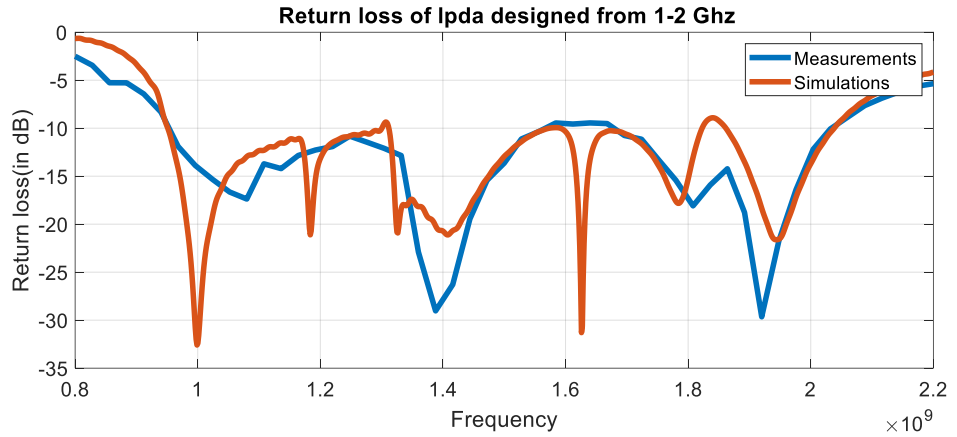


Figure 367- Return loss of the LPDA showing a bandwidth of 1-2 GHz

Finally, the end-fire radiation of the antenna was confirmed by measuring the pattern at 1.2 GHz and 1.8 GHz, as seen in Figures 40 and 41.

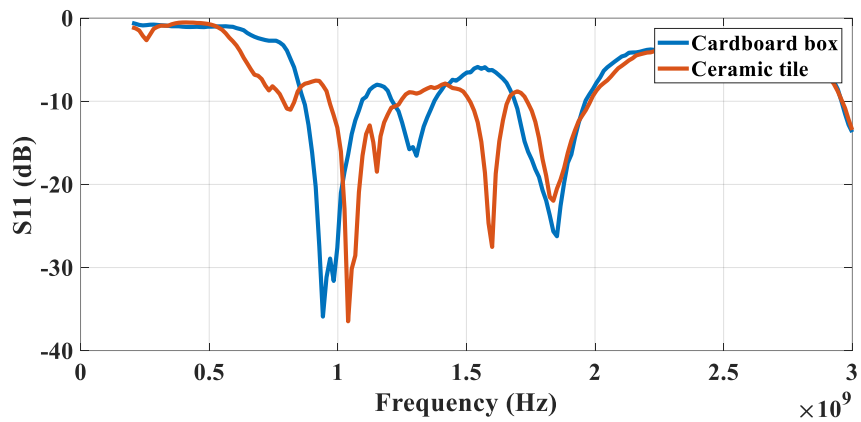


Figure 378 - The LPDA having an affected bandwidth when stuck on cardboard and ceramic tile.

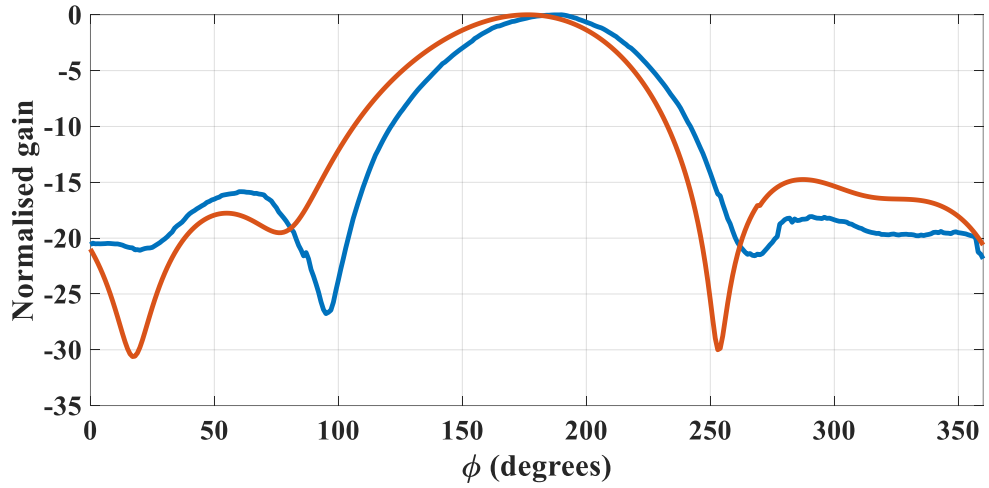


Figure 39 - Radiation pattern for the LPDA at $\theta=90^\circ$, for 1.2 GHz

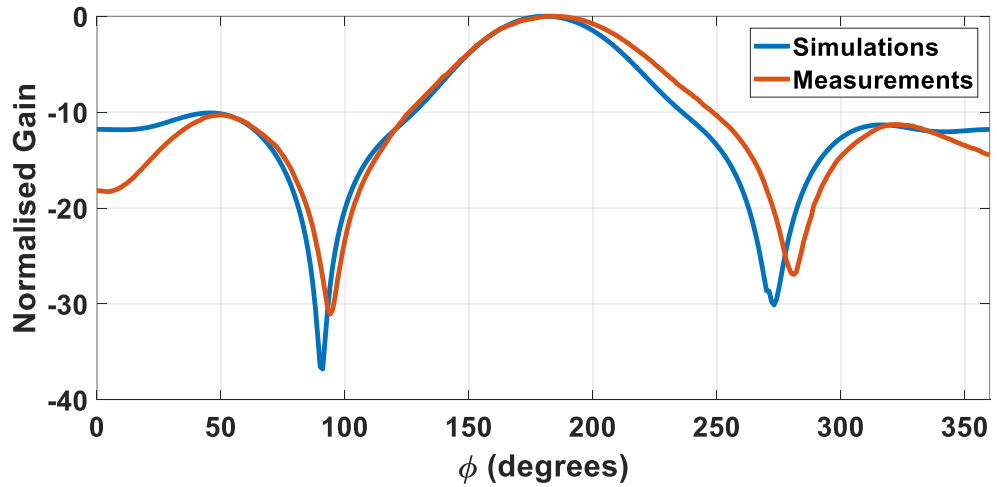


Figure 40 - Radiation pattern for the LPDA at $\theta=90^\circ$, for 1.8 GHz

Next, the second design was fabricated using a CNC machine on a Rogers substrate of thickness 0.78 mm, as seen in Figure 42.



Figure 41 - Fabricated LPDA for bandwidth 300 -1000 MHz

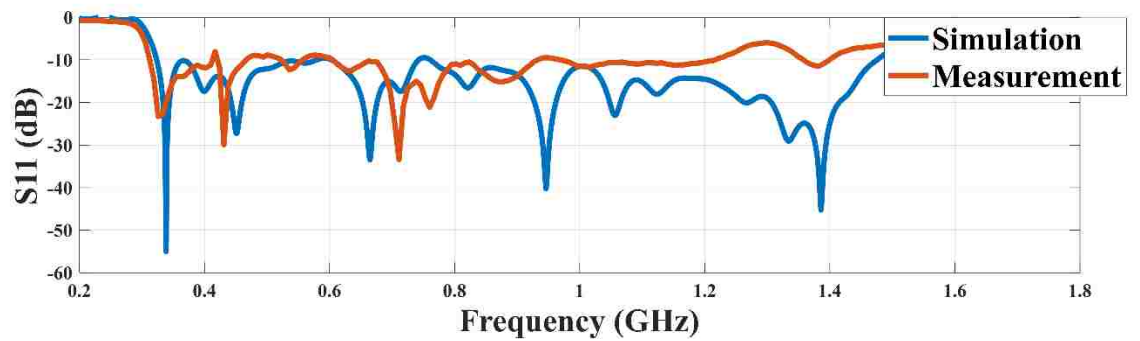


Figure 42 - Return loss measurement and simulation for the LPDA designed from 300-1000 MHz

The bandwidth of this antenna was confirmed using the VNA and is shown in Figure 43. The radiation pattern for the fabricated LPDA was measured and compared to the simulation at 800 and 900 MHz, as seen in Figures 44 and 45.

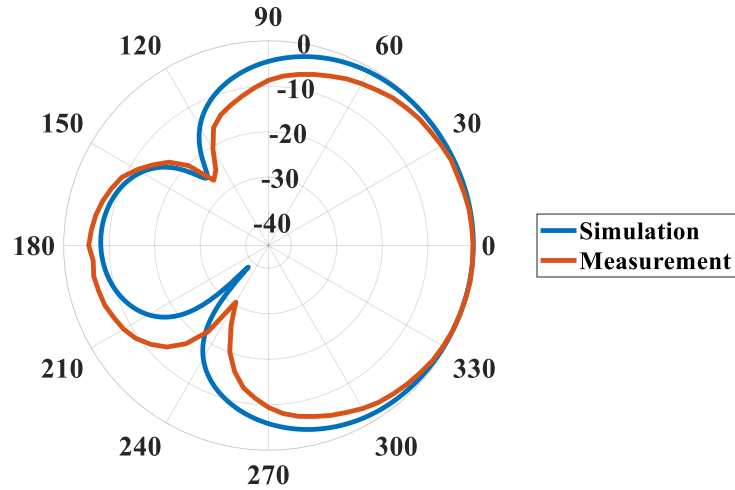


Figure 43 - Radiation pattern for $\theta=90^\circ$, at 800 MHz

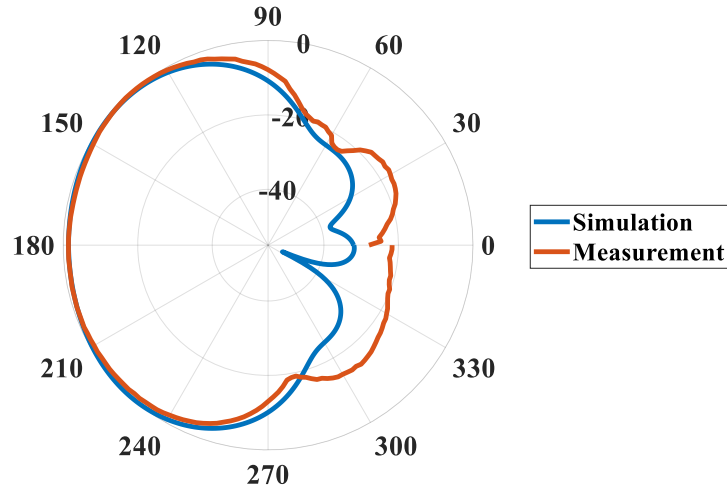


Figure 44 - Radiation pattern for $\theta=90^\circ$, at 900 MHz

The measured gain was found to be 2.99 dB at 800 MHz, and 3.615 dB at 900 MHz. This was in close agreement with the simulation data (3.07 dB at 800 MHz and 2.77 dB at 900 MHz). These values are less than a conventional LPDA and this is probably caused due to the coupling between the elements caused due to meandering.

Also, this LPDA was tested for when stuck on Garolite, a high tensile polymer to replicate the drone like performance, and the results are shown in Figure 46.

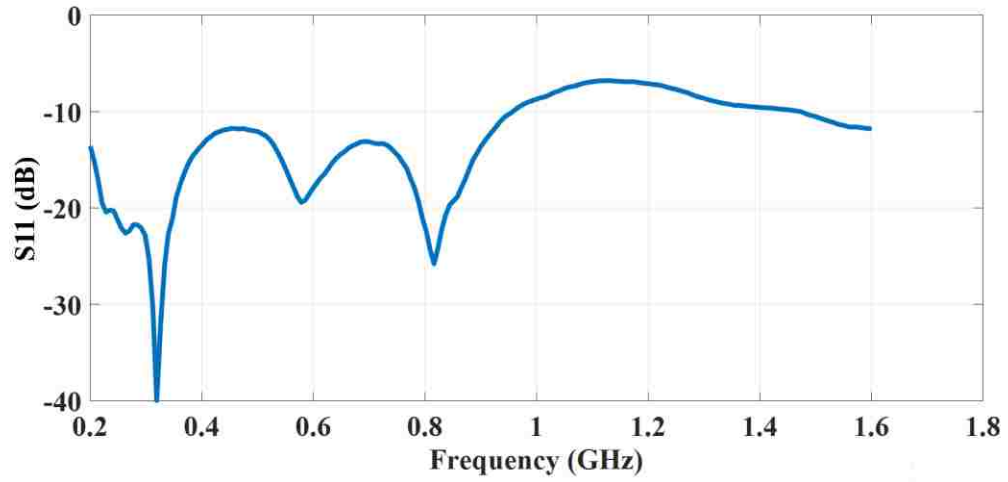


Figure 4538 - Return loss for the LPDA when stuck to Garolite

The bandwidth was seen to be conserved for the required frequency range.

Garolite is made of epoxy resin and is favored in the industry for its high strength and high dimensional stability over temperature.

Chapter 6 – Conclusion

This thesis dealt with the investigation of the possibility of creation of a thin microstrip flexible antenna that could be stuck on any surface and reused by peeling them off after their function was complete. Three types of antennas were tested for this purpose, - a basic annular monopole resonating at a single frequency, a reconfigurable meandering monopole which depending on the external bias works at two different frequencies, and a high bandwidth Log Periodic dipole antenna.

All these antennas were fabricated and tested by being stuck on different surfaces. Certain surfaces caused a shift in the resonance but were deemed to be performing effectively at that particular frequency.

The meandering of the elements of the LPDA effectively miniaturizes the antenna and this was studied to be made more effective by optimizing the Q factor.

For the future the designs need to be tested on conformal surfaces and perhaps even on a structure of a sUAV, to see if they retain the properties even after bending. Also, more different types of adhesives need to be explored which can be more sustainable on repeated usage and can tolerate even more adverse external conditions.

Appendix A – Particle Swarm Optimization

For the optimization technique used to minimize the Q factor of the folded LPDA Particle Swarm Optimization was used, as described in Chapter 3. A.1 describes the algorithm very briefly and A.2 goes through the entire MATLAB code used to link the simulation and conduct a PSO for five parameters with a swarm size of 50 for 50 iterations. It displays the best cost value as its output.

A.1 Theory

The Particle Swarm Optimization (PSO) is a stochastic evolutionary optimization algorithm which was first described in 1997 to describe social behavior.[20] It takes its inspiration from the movement of the members in a flock of birds or a school of fish. It has since then had several applications such as in neural networks, power grid systems, and all sorts of optimization techniques. It extensively aided in the development of a branch of study called swarm intelligence.

In the algorithm, a population of possible solutions(particles) are first initialized via any distribution function. The goal of the system is defined, for which a solution can be obtained for each particle. Once all the solutions are evaluated, the particles are made to move towards a point in the sample space. The movement is guided by two factors – the particles own best position, as well as the whole swarm’s best position. The velocity of each particle with which it is to move can be described by the equation –

$$v_i(t + 1) = wv_i(t) + c_1r_1[x'_i(t) - x_i(t)] + c_2r_2[g(t) - x_i(t)]$$

Here,

i = particle index;

w = inertial coefficient;

c_1, c_2 = acceleration coefficients;

r_1, r_2 = random coefficient, regenerated after every velocity update;

$v_i(t)$ = particle's velocity at time t ;

$x_i(t)$ = particle's position at time t ;

$x'_i(t)$ = particle's individual best position;

$g(t)$ = swarm's best solution

Using this velocity, each particle has its position updated using the equation –

$$x_i(t + 1) = x_i(t) + v_i(t + 1)$$

This whole process is repeated till the maximum number of iterations is reached, giving us the best solution for that particular swarm size and number of iterations.

There are various schools of thought as to how this entire process leads to optimization, since there is no mathematical guarantee that the best solution will be obtained.

PSO has been already used in antennas [21] to optimize antennas with goals such as suppressing side lobes or obtaining nulls in certain positions. The vast appeal

towards PSO is due to its ease of understanding, and the easy computations. However, the major drawback of this algorithm is that since it does not involve any gradient descent, it can never guarantee the optimum solution.

A.2 MATLAB Code

```

CST = actxserver('CSTStudio.Application');%interface to access CST from MATLAB%
mws = CST.invoke('Active3D');
solv=mws.invoke('Solver');
plot1d=mws.invoke('Plot1d');
export=mws.invoke('ASCIIExport')
mws.invoke('OpenFile','C:\Users\Jay\Dropbox\Final models\Lpdafinal1.cst');%File
location to be inserted%
solv.invoke('Start');
exportpathr = 'C:\Users\Jay\Documents\MATLAB\CST_App-master\CST_App\Zreal.txt'
exportpathi = 'C:\Users\Jay\Documents\MATLAB\CST_App-master\CST_App\Zimag.txt'
filenameTXT1 = 'Zreal';
filenameTXT2 = 'Zimag';
CstExportZparametersrealTXT(mws, exportpathr);
CstExportZparametersimagTXT(mws, exportpathi);
[ Freq, Zreal] = textread('Zreal.txt', '%f %f','headerlines', 2);
[ Freq, Zimag] = textread('Zimag.txt', '%f %f','headerlines', 2);
omega=2*pi*Freq;
dr= diff(Zreal)./diff(Freq);
dx= diff(Zimag)./diff(Freq);
Cost = 0;
for(i=1:1000)
    Q(i)=(omega(i)/(2*Zreal(i)))*sqrt((dr(i)^2)+(dx(i)+abs(dx(i)/omega(i)))^2);
    Cost = Cost + Q(i);
end

```

```

%% PSO begins

nVar = 5;

VarSize = [1 nVar]; % This is just the size of the matrix to be used in whole code %

C1=mws.invoke('GetParameterNValue','1'); % The exact parameter number has to be
found out by trial and error%

C2=mws.invoke('GetParameterNValue','2');

C3=mws.invoke('GetParameterNValue','3');

C4=mws.invoke('GetParameterNValue','4');

C5=mws.invoke('GetParameterNValue','5');

VarMin = [20 18 18 15 15]; % Lower Bound of Decision Variables%

VarMax = [15 15 15 10 10]; % Upper Bound of the variable%

%% Parameters of PSO

MaxIt = 50; %Maximum number of iterations

nPop = 50; % Population size

w = 1;      % Inertia Coefficient

wdamp = 0.99; % Damping Ratio of Inertia Coefficient

c1 = 2;     % Personal Acceleration Coefficient

c2 = 2;     % Social Acceleration Coefficient

%%Initialization

% The Particle Template

empty_particle.Position = [];

empty_particle.Velocity = [];

empty_particle.Cost = [];

empty_particle.Best.Position = [];

empty_particle.Best.Cost = [];

% Initialize Global Best

GlobalBest.Cost = inf;

MaxVelocity = 0.2*(VarMax-VarMin);

MinVelocity = -MaxVelocity;

```

```

% Initialize Population Members
for i=1:nPop
    % Generate Random Solution
    particle(i).Position = unifrnd(VarMin, VarMax, VarSize);
    % Initialize Velocity
    particle(i).Velocity = zeros(VarSize);
    % Evaluation
    Temp = particle(i).Position
    cost = Estimation(mws,Temp);
    particle(i).Cost = cost;
    % Update the Personal Best
    particle(i).Best.Position = particle(i).Position;
    particle(i).Best.Cost = particle(i).Cost;
    % Update Global Best
    if particle(i).Best.Cost < GlobalBest.Cost
        GlobalBest = particle(i).Best;
    end
end
end
% Array to Hold Best Cost Value on Each Iteration
BestCosts = zeros(MaxIt, 1);
%% Main Loop of PSO
for it=1:MaxIt
    for i=1:nPop
        % Update Velocity
        particle(i).Velocity = w*particle(i).Velocity ...
            + c1*rand(VarSize).*(particle(i).Best.Position - particle(i).Position) ...
            + c2*rand(VarSize).*(GlobalBest.Position - particle(i).Position);
        % Apply Velocity Limits
        particle(i).Velocity = max(particle(i).Velocity, MinVelocity);
        particle(i).Velocity = min(particle(i).Velocity, MaxVelocity);
    end
end

```

```

% Update Position
particle(i).Position = particle(i).Position + particle(i).Velocity;
% Apply Lower and Upper Bound Limits
particle(i).Position = max(particle(i).Position, VarMin);
particle(i).Position = min(particle(i).Position, VarMax);
%Evaluation
Temp = particle(i).Position
cost = Estimation(mws,Temp);
particle(i).Cost = cost;
% Update Personal Best
if particle(i).Cost < particle(i).Best.Cost
    particle(i).Best.Position = particle(i).Position;
    particle(i).Best.Cost = particle(i).Cost;
    % Update Global Best
    if particle(i).Best.Cost < GlobalBest.Cost
        GlobalBest = particle(i).Best;
    end
end
end
end
% Store the Best Cost Value
BestCosts(it) = GlobalBest.Cost;
% Display Iteration Information
disp(['Iteration ' num2str(it) ': Best Cost = ' num2str(BestCosts(it))]);
% Damping Inertia Coefficient
w = w * wdamp;
end

```

References

- [1] Army PM UAS Spectrum Update. (2012). [online] Available at: <https://apps.dtic.mil/tr/fulltext/u2/a567397.pdf> [Accessed 13 Jan. 2019].
- [2] Chu, L. (1948). Physical Limitations of Omni-Directional Antennas. *Journal of Applied Physics*, 19(12), pp.1163-1175.
- [3] Yaghjian, A. and Best, S. (2005). Impedance, bandwidth, and Q of antennas. *IEEE Transactions on Antennas and Propagation*, 53(4), pp.1298-1324.
- [4] Wheeler, H. (1947). Fundamental Limitations of Small Antennas. *Proceedings of the IRE*, 35(12), pp.1479-1484.
- [5] Volakis, J., Chen, C. and Fujimoto, K. (2010). *Small antennas*. New York: McGraw-Hill.
- [6] Fante, R. (1969). Quality factor of general ideal antennas. *IEEE Transactions on Antennas and Propagation*, 17(2), pp.151-155.
- [7] Collin, R. and Rothschild, S. (1964). Evaluation of antenna Q. *IEEE Transactions on Antennas and Propagation*, 12(1), pp.23-27.
- [8] J. S. McLean, "A re-examination of the fundamental limits on the radiation Q of electrically small antennas," *IEEE Transactions on Antennas and Propagation*,

vol. AP-44, May 1996, pp. 672-675.

[9] S. R. Best, "A discussion on power factor, quality factor, and efficiency of small antennas," IEEE International Symposium on Antennas and Propagation, June 2007, pp. 2269-2272.

[10] H. T. Nguyen, S. Noghianian, and L. Shafai, "Microstrip patch miniaturization by slots loading," IEEE Antennas and Propagation Society International Symposium, 2005, pp. 215-218.

[11] J. Rashed-Mohassel, A. Mehdipour, and H. Aliakbarian, "New schemes of size reduction in space filling resonant dipole antennas," 3rd European Conference on Antennas and Propagation, vol. 23-27, 2009, pp. 2430-2432.

[12] M. C. Scardelletti, G. E. Ponchak, S. Merritt., J. S. Minor, and C. A. Zorman, "Electrically small folded slot antenna utilizing capacitive loaded slot lines," IEEE Radio and Wireless Symposium, vol. 22-24, 2008, pp. 731-734.

[13] Y. Tawk, A. El-Amine, S. Saab, J. Costantine, F. Ayoub and C. G. Christodoulou, "A Software-Defined Frequency-Reconfigurable Meandered Printed Monopole," in IEEE Antennas and Wireless Propagation Letters, vol. 17, no. 2, pp. 327-330, Feb. 2018.

[14] R. H. DuHamel and D. E. Isbell, "Broadband Logarithmically Periodic Antenna Structures," 1957 IRE National Convention Record, Part 1.

- [15] R. L. Carrell, "The Design of Log-Periodic Dipole Antennas," 1961 IRE International Convention Record, Part 1.
- [16] Pantoja, R., Sapienza, A. and Filho, F. (1987). A microwave printed planar log-periodic dipole array antenna. *IEEE Transactions on Antennas and Propagation*, 35(10), pp.1176-1178.
- [17] Ntia.doc.gov. (2019). [online] Available at: https://www.ntia.doc.gov/files/ntia/publications/compendium/0960.00-1164.00_01MAR14.pdf [Accessed 11 May. 2019].
- [18] Tape, C. (2019). *Pressure Sensitive Adhesive Tape (PSA) and it's Advantages*. [online] Can-Do National Tape. Available at: <https://www.candotape.com/adhesive-tape-consultant/pressure-sensitive-adhesive-tape/> [Accessed 19 Apr. 2019].
- [19] Industries, A. (2019). *uFL SMT Antenna Connector*. [online] Adafruit.com. Available at: <https://www.adafruit.com/product/1661> [Accessed 22 May 2019].
- [20] Kennedy, J.; Eberhart, R. (1995). "Particle Swarm Optimization" Proceedings of IEEE International Conference on Neural Networks. IV. pp. 1942–1948.
- [21] Khodier, M. and Christodoulou, C. (2005). Linear array geometry synthesis with minimum sidelobe level and null control using particle swarm optimization. *IEEE Transactions on Antennas and Propagation*, 53(8), pp.2674-2679.